IV International Seminar on ORC Power Systems, ORC2017
13-15 September 2017, Milano, Italy

Optimal Aerodynamic Design of a Transonic Centrifugal Turbine Stage for Organic Rankine Cycle Applications

Giacomo Persico*, Vincenzo Dossena, Paolo Gaetani

Laboratorio di Fluidodinamica delle Macchine, Dipartimento di Energia, Politecnico di Milano, Via Lambruschini 4, Milano, 20156, Italia

Abstract

This paper presents the results of the application of a shape-optimization technique to the design of the stator and the rotor of a centrifugal turbine conceived for Organic Rankine Cycle (ORC) applications. Centrifugal turbines have the potential to compete with axial or radial-inflow turbines in a relevant range of applications, and are now receiving scientific as well as industrial recognition. However, the non-conventional character of the centrifugal turbine layout, combined with the typical effects induced by the use of organic fluids, leads to challenging design difficulties. For this reason, the design of optimal blades for centrifugal ORC turbines demands the application of high-fidelity computational tools. In this work, the optimal aerodynamic design is achieved by applying a non-intrusive, gradient-free, CFD-based method implemented in the in-house software FORMA (Fluid-dynamic OptimizeR for turboMachinery Aerofoils), specifically developed for the shape optimization of turbomachinery profiles. FORMA was applied to optimize the shape of the stator and the rotor of a transonic centrifugal turbine stage, which exhibits a significant radial effect, high aerodynamic loading, and severe non-ideal gas effects. The optimization of the single blade rows allows improving considerably the stage performance, with respect to a baseline geometric configuration constructed with classical aerodynamic methods. Furthermore, time-resolved simulations of the coupled stator-rotor configuration shows that the optimization allows to reduce considerably the unsteady stator-rotor interaction and, thus, the aerodynamic forcing acting on the blades.

Keywords: Centrifugal turbine; ORC power systems; shape-optimization; evolutionary algorithm; stator-rotor interaction; aerodynamic forcing

1. Introduction

Among the several industrial application of organic fluids, Organic Rankine Cycle (ORC) power systems represent one of the most attractive technology for the exploitation of energy sources featuring medium-low enthalpy level [1]. As well known ([2],[3]), the performance of the whole ORC power system is crucially determined by the efficiency of the turbine, whose optimization is complicated by the character of organic fluids, which combine low enthalpy drops with high expansion ratios. The low enthalpy drop has historically led to compact configurations with relatively low number of stages, featuring supersonic flows, converging-diverging cascades and strong shocks at blade outlet

---

* Corresponding author. Tel.: +39-02-2399-8605
  E-mail address: giacomo.persico@polimi.it

regions [4,5]. The subsequent limitations in the design and (especially) off-design turbine performance call for layouts featuring higher number of stages in present-day ORC turbines, accepting an increased size of the machine.

With the aim of preserving compactness while increasing the number of stages, the novel radial-outflow or centrifugal turbine represents a valid alternative to conventional layouts, and it is now receiving scientific [6] as well as industrial [7] recognition. The centrifugal layout allows disposing many stages in a relatively compact device, reducing the cascade expansion ratios and, hence, avoiding supersonic flow conditions. Furthermore, centrifugal turbines can properly accomplish the large volumetric flow ratio thanks to the inherent increase of passage area along the flow path, thus limiting the flaring angle without significant increase in meridional flow component. For these reasons, this set-up has the potential for achieving high aerodynamic performance as well as wide power control capability.

A research program on the development of novel centrifugal turbines for ORC applications is presently ongoing at Politecnico di Milano, with the aim to propose specific design remarks for this technology. To this end, a design methodology has been conceived with a hierarchical approach, first considering the preliminary design on the basis of mean-line and throughflow codes [6], then laying-down basic criteria for the aerodynamic design of centrifugal turbine profiles [8], and finally focusing on the three-dimensional aerodynamics of centrifugal turbine blade rows [9].

As a step forward of this study, the optimal design of a centrifugal turbine stage (considering both the stator and the rotor blades) is proposed in the present paper. Due to the non conventional configuration, the identification of the optimal shapes for centrifugal turbine blades working with organic fluids demands the application of an automated and systematic technique based on high-fidelity computational tools and optimization strategies. The procedure here applied is constructed by combining a geometrical parametrization technique, a Computational Fluid Dynamic (CFD) model, and a surrogate-based gradient-free optimization method. High-fidelity steady and time-resolved calculations of the flow in the stage are then performed for both the baseline and optimal configurations, to investigate the effects of optimization on both the stage efficiency and the aerodynamic forcing acting on the front section of the rotor blade.

This paper is structured as follows. At first the stage configuration and the construction of the baseline configuration for the turbine blades are recalled. Then the shape optimization of the two blades is presented. Finally the unsteady flow in the baseline and optimal configurations, as well as the stage performance, are presented and discussed.

2. Baseline Blade Configuration

The centrifugal blade rows studied in this work were conceived for application in the six-stage ORC centrifugal turbine proposed in [6] operating with MDM as working fluid. Operating conditions, size, power release, and aerodynamic efficiency resulting from the preliminary design were discussed in [6] and are recalled here in Table 1.

Table 1. 6-stage turbine conditions, size and performance.

Fluid	$P_{T,in}$	$T_{T,in}$	P_{out}	Ω	Outlet Diameter	Power	Total-to-total efficiency
MDM	10 bar	274 C	0.17 bar	3000 rpm	1.0 m	1.27 MW	0.869

The layout of the turbine consists in six 0.5 reaction stages, each of them featuring the same discharge flow angle (66.7 deg, opposite in sign between stators and rotors), and the same blade meridional chord (26 mm). The six-stage arrangement allows to limit the flow regime to transonic conditions, despite the large pressure ratio.

The present work discusses the optimal aerodynamic design of the first-stage nozzle and rotor blade rows, refereed to as CN-I and CR-I in the following. As usual in present-day turbomachinery design, simple criteria are first applied to identify a preliminary shape configuration, which is then optimized using an automatic technique. In the present study, the preliminary (or baseline) shape of the two blade profiles were obtained by applying the technique proposed in [8], which suggests to adopt aft-loaded profiles featuring an elliptic-arc mean line to provide a sufficiently smooth acceleration of the flow along the blade channel. Then, a conventional distribution of thickness is applied to the mean-line to construct the blade. The resulting profiles, originally constructed in the Cartesian coordinate system, are finally mapped on the polar one using a conformal transformation, in order to maintain the geometric angles of the blade.

Figure 1 reports the layout of the two blade rows under consideration, obtained by applying the aforementioned procedure. The CN-I blade was constructed in order to deflect the flow from radial-outward flow to 66.7 deg; the blade number, selected using the Zweifel criterion, resulted equal to 27. The distribution of thickness was taken from
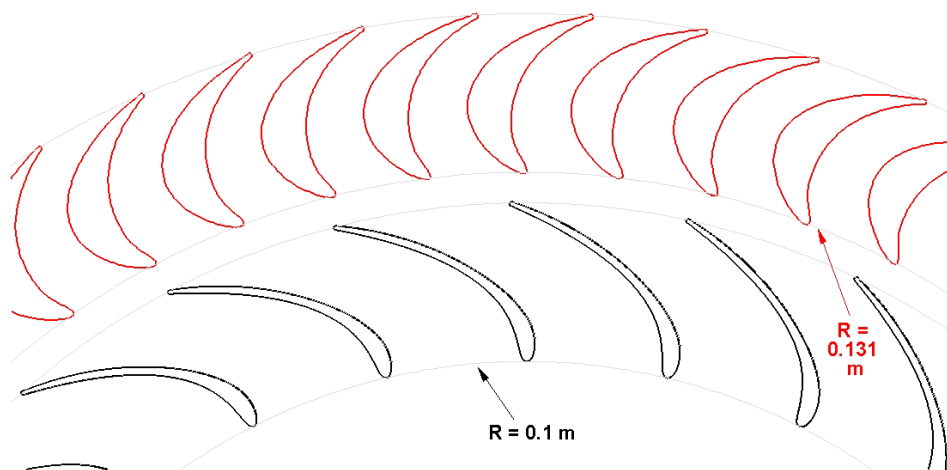
Fig. 1. Baseline configuration of the CN-I (in black) and the CR-I (in red) blade rows assembled in the first stage of the centrifugal turbine.

that of a lightly loaded low-pressure axial turbine. The CR-I blade was constructed to deflect the (relative) flow from about +50 deg to -66.7 deg; for such a high aerodynamic loading, the application of the Zweifel criterion led to 52 blades. Moreover, the slender profile shape used for the stator was found to be unsuitable for a blade with turning larger than 90 deg, as flow-detachment might occur in the central part of the profile. For this reason an alternative thickness distribution was assigned, taken from that of a high-pressure turbine blade, resulting in a more advantageous configuration also from te structural point of view.

3. Blade Optimization

The progress in computational capability, the increased fidelity of CFD models, and the improved effectiveness of optimization algorithms have recently triggered the development of novel design tools to determine the optimal shape of turbomachinery blades. Among the techniques presently available, deterministic adjoint-based methods [10,11] and heuristic evolutionary methods [12] are nowadays object of intense application and research in Aerodynamics. Evolutionary methods, in particular, are of interest as they allow to explore a wide range of feasible solutions without being 'intrusive' with respect to the source flow model, as they only require the use of direct calculation tools.

In this work, the shape-optimization of the centrifugal blades is carried out by applying the in-house package FORMA (Fluid-dynamic OptimizeR for turbo-Machinery Aerofoils) recently set-up at Politecnico di Milano. The optimization strategy, introduced in the following, is constructed by combining three main bricks, i.e. a geometry-parameterization code, a high-fidelity and validated CFD solver, and a surrogate-based evolutionary algorithm.

3.1. Geometry Parameterization Method

In shape optimization problems, it is common practice to parametrize the geometry with piecewise functions, so to control the shape by moving a limited number of so-called Control Points (CPs). In the FORMA package, B-Spline curves are used to parameterize the line of the blade profile; the global and local control of the shape provided by the use of B-Splines makes them a powerful tool for aerodynamic design [13]. The position of the CPs and their range of variation define the design space of the optimization problem. Piecewise lines of order 3 are used in this work. More details on the parametrization technique can be found in [14].

To set-up the optimization, at first an approximate representation of the baseline blade shape is constructed using a B-Spline curve, defined and manipulated by the position of the CPs; once the number and the spacing of the CPs is prescribed, the coordinates of the CPs are found via a least squares interpolation method. The pressure and suction sides of the blade are generated as a unique B-Spline curve, filleted by a circular-arc trailing edge.

3.2. Computational Flow Model

To evaluate the fitness of the configurations progressively selected by the optimization algorithm, quasi-3D CFD simulations are performed using the ANSYS-CFX solver. Turbulence effects are introduced using the $k - \omega\ SST$ model, prescribing wall y^+ below unity all along the blade profile. To introduce the non-ideal thermodynamic behavior of the MDM, a look-up table approach was used. The look-up table was constructed by sampling the Span-Wagner Equations of State [15] though the thermodynamic library *FluidProp* and including tabulated transport properties.

Calculations are performed on structured grids composed by hexahedral elements, re-generated for each CFD run performed throughout the optimization process. Meshes composed by 50 kcells in the blade-to-blade surface were found to provide an optimal trade-off between computational cost (10 minutes for a CFD run on a 16-processor Linux cluster) and result fidelity (5% overestimate in the entropy production with respect to the grid independent value [8]).

The baseline and optimal configurations were finally assessed after the optimization by means of time-resolved CFD simulations performed on a grid independent mesh (composed by 100 kcell in the blade-to-blade surface) and using second order accuracy for the discretization of the unsteady term. The reliability of the time-resolved flow model had been previously assessed against unsteady measurements performed by the authors themselves [16].

3.3. Surrogate-Based Optimization Strategy

The optimization technique applied in this work is based on Genetic Algorithms (GAs). GAs are attractive as they allow to deal with oscillating and non-smooth objective functions, as well as to easily handle constrained and multi-objective optimization problems [17]. Furthermore, GAs are global optimization methods and, hence, are best suited in presence of a multiplicity of local optima (a situation that cannot be excluded a priori in aerodynamic design).

Nevertheless, GAs require a massive application of the direct computational tool, that in case of CFD often result in an unacceptable computational burden. To tackle this cost, a surrogate evolutionary strategy was applied in this study. This technique is conceived so that the GA operates only on a surrogate model of the objective function. To be effective, the surrogate model has to be a reliable representation of the objective function; in surrogate-based strategies the model is initialized and progressively updated during the optimization, so that the shape is optimized while the reliability of the surrogate improves. In this work, the objective function is approximated by applying the the Kriging meta-model, as it allows to properly capture the complexity of response surfaces featuring sharp curvature changes, even in presence of highly irregular distributions of interpolation points.

In surrogate-based optimization, the model is initialized by interpolating a database of configurations tested with CFD. To improve the reliability of the surrogate model, a Surrogate-Based Global Optimization (SBGO) is applied. In SBGO, the model is 'trained' by progressively adding the optima found during the optimization, and tested with CFD, to the initial database. In this way, the SBGO results computationally efficient, even though the convergence is not guaranteed. However, previous applications of FORMA [14,18] as well as preliminary trials made at the early stages of this work did not show convergence issues if a sufficiently large initial data-base is assigned.

The FORMA package was assembled making use of the object-oriented framework Dakota [19]. A single-objective GA was used as optimization tool, by resorting to the JEGA library (Java Engine for Genetic Algorithms). After a preliminary parametric study, the GA was set-up with a population size of 300 generations, a crossover rate of 0.8, and a mutation rate of 0.02; elitism was also used as a selection technique. To determine the Kriging parameters, the Surfpack library was employed. In order to initialize the surrogate model, a Latin Hypercube technique was used, with a population equal to 10 times the number of design variables.

3.4. Optimization results

In this work the FORMA package was applied to optimize singularly the blades of the CN-I and the CR-I cascades. The performance of the resulting stage was then evaluated afterwards, by combining the optimal cascades. The CN-I case is first considered, then the CR-I case is presented.

Despite the moderate level of cascade aerodynamic loading, the design of CN-I is complicated by the significant radial effect. The application of the design method proposed in [8] to CN-I leads to blades featuring a long and curved region of un-guided turning on the rear suction side. This makes critical the blade aerodynamics, especially considering the transonic flow regime, which may lead to the onset of shocks in the rear part of the profile (see [9]).
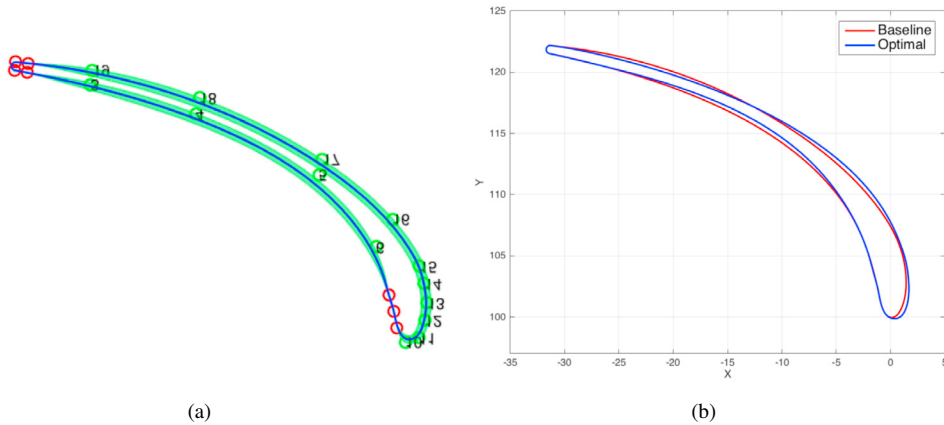
(a) (b)

Fig. 2. CN-I optimization. (a): design space definition. (b) baseline and optimal shapes

To proper control the CN-I blade aerodynamics, the shape optimization was focused on the rear part of the profile. However, as discussed in detail in [18], also the front suction side was found to be critical, as adverse pressure gradients might establish in this area. Therefore, the CN-I baseline geometry was parametrized with 21 CPs, 14 of those are movable by $\pm 0.4 mm$ along the direction normal to the local blade surface, as reported in Figure 2(a). The optimization was run by assigning the entropy generation across the cascade as objective function to minimize. Figure 2(b) reports the result of the optimization by comparing the baseline and the optimal blade shapes. The optimization enlarges the blade in the leading edge region, it increases the blade curvature in the central region, and finally it reduces the curvature in the rear region downstream of the throat (thus limiting the un-guided turning). This shape allows to minimize the over-speed on the rear suction side and the subsequent rear shock, and also guarantees a smooth pressure distribution along the whole blade surface. In quantitative terms, the optimization reduces by about 35% the entropy production. Single-cascade CFD simulations with grid-independent mesh indicates a drop from 3.1% to 2.0% in kinetic energy loss coefficient (here defined as the isentropic-to-real enthalpy difference at the cascade exit divided by the discharge kinetic energy, both evaluated at 20% of the radial chord downstream of trailing edge).

CR-I exhibits very different features with respect to CN-I, but it shares with this latter some design difficulties; the significant curvature in the rear region, required to regularly distribute the very high turning along the whole blade, complicates the design especially on the suction side. The 'crown' region in the central section of the blade, featuring the largest camber and the largest thickness of the blade, is also critical, especially for the control of blade loading. These considerations led to parametrize the blade with 20 CPs, 8 of those are movable by $\pm 1mm$ along the direction
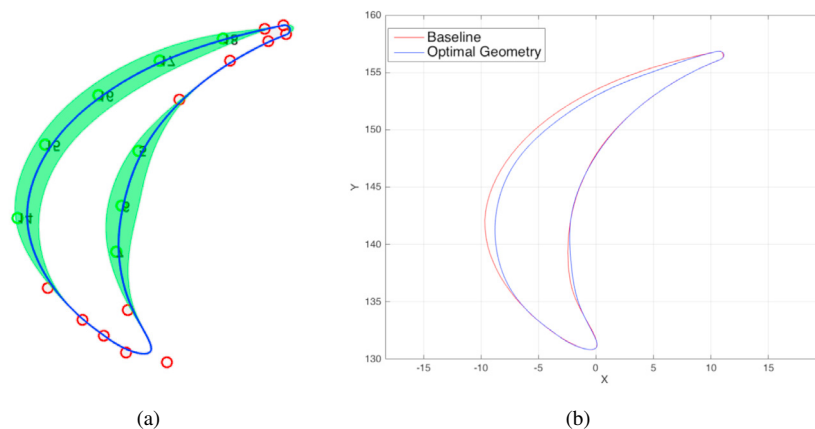

(a) (b)

Fig. 3. CR-I optimization. (a): design space definition. (b) baseline and optimal shapes

normal to the local blade surface, as reported in Figure 3(a). Figure 3(b) reports the comparison between the baseline and the optimal rotor blade shape. The optimization alters significantly the rear suction side of the blade, reducing the curvature in the region of un-guided turning. The optimization also reduces the blade thickness in the 'crown' region of the blade, leaving instead almost unaltered the pressure side of the blade. As a result, the flow turning process within the channel is smoothed and the shock generated in the rear suction side is weakened. In quantitative terms, the optimization reduces the entropy production by about 50%; the resulting kinetic energy loss coefficient, evaluated half a radial chord downstream of trailing edge by means of single-cascade CFD simulations in the rotating frame, drops from 5.9% to 2.8%.

4. Stage performance

The optimization of the stator and rotor blades leads to a net reduction of entropy generation across the cascades. The increase in stage performance provided by the optimization can be properly quantified by means of stator-rotor coupled simulations. For this analysis, the configuration with the baseline blades (namely, the one shown in Figure 1) was compared with the stage featuring the optimal blades. The stage performance, evaluated as total-to-total efficiency, was found to increase from 92.0% to 93.2% when optimal blades are adopted. This difference is sufficiently high for being estimated reliably by the CFD solver (as demonstrated against experiments in [16]), and confirms that a significant increase in stage performance can be achieved by applying optimization tools to centrifugal turbines.

5. Stage unsteady aerodynamics

To appreciate the impact of optimization with a more broad perspective, the time-resolved aerodynamics of the stage configuration is now considered. In particular, two simulations were performed, by considering first the baseline stator and then the optimal stator in combination to the optimal rotor. In this way, the impact of the stator blade optimization on the rotor aerodynamics can be highlighted. As the rotor blade number is not an exact multiple of the stator one, the rotor blade was scaled by applying a homothetic transformation, so to match the closest multiple of stator blade number (54) keeping unaltered the blade shape.

Figure 4 reports the instantaneous distributions of absolute Mach number in the whole stage for the case with the baseline stator at four instants of the rotor blade passing period (BPP in the following). Such images allow to highlight the shock patterns in-between the blade rows, as well as their impact on the stator aerodynamics in the region of un-guided turning and on the rotor aerodynamics in the front section of the blade. As a general consideration, the aerodynamic interaction between the blade rows is very significant, as a result of the transonic nature of the flow and the very small radial gap. In particular, from the beginning ($t/BPP = 0.00$) to the middle ($t/BPP = 0.50$) of the BPP, the flow evolves from a smooth shock-free condition into a configuration featuring a region of supersonic flow, where the Mach number reaches 1.25, followed by a relatively strong shock impinging on the front section of the rotor blade. The observed evolution of the flow is motivated by the combination between the local expansion regions on the stator and rotor blades. As the rotor sweeps in front of the stator, a diverging 'virtual' duct is generated in-between the rear suction side of the stator and the front suction side of the rotor, promoting the supersonic expansion of the transonic flow discharged by the stator; the shape (in particular, the cross-section variation) of this virtual duct changes with time, altering the instantaneous Mach number distribution in this region. Similar effects were observed in transonic axial gas turbines [20,21]; however, the shape of the virtual duct (and its change with time) is much more difficult to visualize and identify in the present centrifugal layout, as the radial effect makes the cross-section to inherently increase in the stator-rotor gap. In the second half of the period ($t/BPP = 075$) the relative position of stator and rotor determines a virtual duct with a very small divergence, resulting in a lower over-speed and a weakening of the shock.

The frames of Figure 4 indicate that the non-optimized stator induces large fluctuations on the rotor loading. To highlight the impact of optimization on the rotor aerodynamic forcing, Figure 5 reports the same kind of representation of Figure 4, but for the stage with both optimal stator and rotor cascades. The flow phenomena and the evolution of the flow are similar to those described for the previous case; nevertheless, the optimization of the stator blade leads to a significant reduction of the over-speed generated in the stator-rotor gap. In the central part of the BPP the supersonic flow region within the virtual duct constituted by the stator and rotor blades still appears, but with a lower maximum Mach number(1.15 against 1.25 of the previous case). Single-cascade simulations show that the optimization reduces
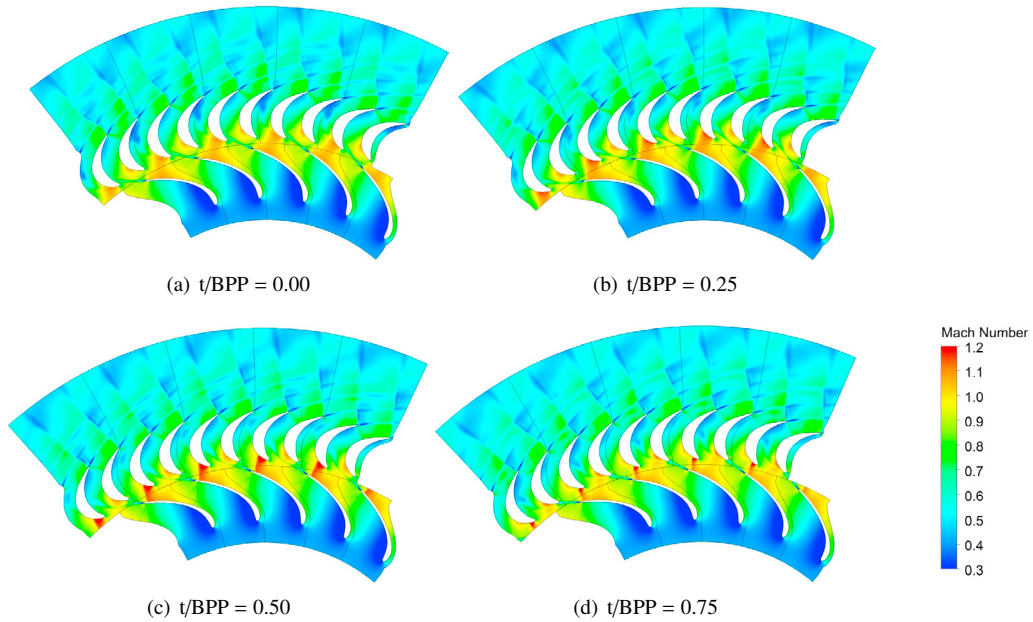
(a) t/BPP = 0.00

(b) t/BPP = 0.25

(c) t/BPP = 0.50

(d) t/BPP = 0.75

Fig. 4. Centrifugal turbine with baseline stator and the optimal rotor. Instantaneous Mach number distribution.

(a) t/BPP = 0.00
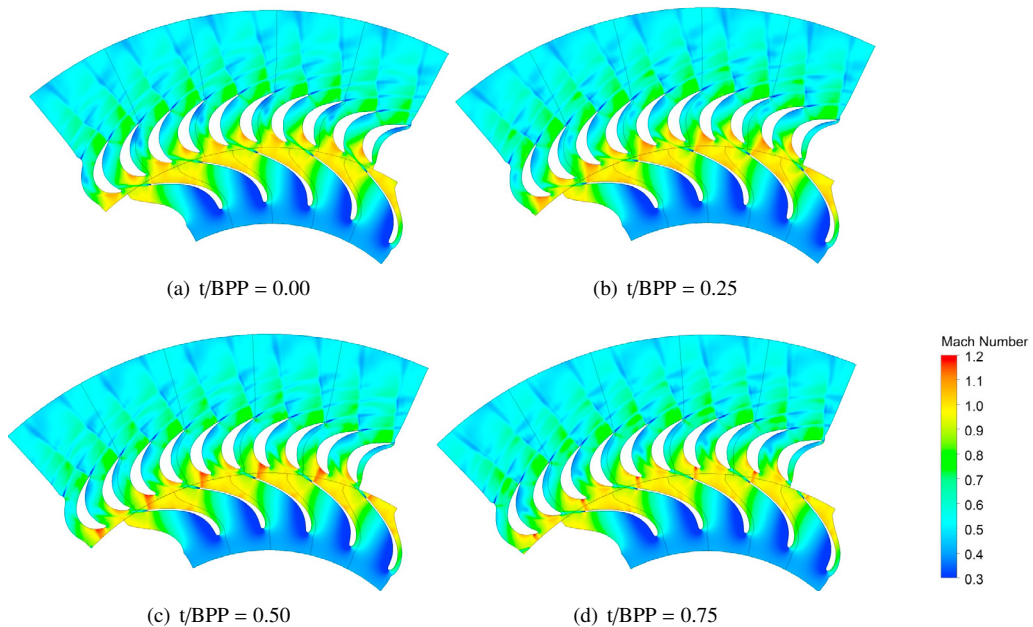
(b) t/BPP = 0.25

(c) t/BPP = 0.50

(d) t/BPP = 0.75

Fig. 5. Centrifugal turbine with optimal stator and rotor blades. Instantaneous Mach number distribution.

the over-speed of the stator blade; this beneficial feature is preserved when the cascade is operated in the actual unsteady condition of the stage, leading to a weaker shock impinging on the rotor and thus reducing the forcing.

Alongside stator-rotor interaction effects, the optimization may have an impact also on the interaction between the stages. As visible from the sharp gradients in absolute Mach number downstream of the turbine, the rotor itself is transonic and generates a relatively strong shock close to the trailing edge, modulated by the interaction with the wake and pressure field of the first stator. The optimization of the CR-I weakens the shock as well as the optimization of the CN-I reduces the shock modulation, potentially minimizing the forcing on the blade rows of the following stage.

6. Conclusions

This paper has presented the application of a shape-optimization technique to the design of a centrifugal turbine stage for ORC application. The technique, implemented in the in-house design package FORMA, makes use of a geometry-parametrization tool, an high-fidelity flow solver, and a surrogate-based evolutionary algorithm.

The baseline shape of the blades, constructed by means of conventional aerodynamic methods, were first parametrized via B-Splines identified by a limited number of control points. An experimentally validated CFD model was used in combination to a look-up table approach for the simulations of non-ideal transonic flow of organic fluids. To tackle the computational cost of the optimization, the evolutionary algorithm was coupled to a Kriging surrogate model.

The study has demonstrated that the application of an automated method to optimize the shape of non-conventional blade rows provides relevant benefits in terms of stage efficiency, which rises by more than 1%, and of aerodynamic forcing. As a matter of fact, the optimization of the blades reduces both the entropy generation and the azimuthal gradients in the flow released by the cascades, weakening the stator-rotor interaction phenomena. This results in weaker shocks impinging on the rotor blade and weaker shocks generated at the rotor-exit, reducing the flow unsteadiness.

References

[1] Gaia, M.. 30 Years of Organic Rankine Cycle Development. In: First International Seminar on ORC Power Systems, Keynote Lecture. 2011,.
[2] Macchi, E.. The Choice Of Working Fluid: The Most Important Step For A Successful Organic Rankine Cycle (And An Efficient Turbine). In: Second International Seminar on ORC Power Systems, Keynote Lecture. 2013,.
[3] La Seta, A., Meroni, A., Andreasen, J.G., Pierobon, L., Persico, G., Haglind, F.. Combined Turbine and Cycle Optimization for Organic Rankine Cycle Power SystemsPart B: Application on a Case Study. Energies 2016;9(393).
[4] Hoffren J., T.T., Larjola, J., Siikonen, T.. Numerical Simulation of Real-Gas Flow in a Supersonic Turbine Nozzle Ring. ASME J Eng Gas Turb Power 2002;124:395–403.
[5] Harinck, J., Colonna, P., Guardone, A., Rebay, S.. Influence of thermodynamic models in 2D flow simulations of turboexpanders. ASME J Turbomach 2010;132:pp. 011001–17.
[6] Pini, M., Persico, G., Casati, E., Dossena, V.. Preliminary design of a centrifugal turbine for ORC applications. ASME J Eng Gas Turb Power 2013;135(042312).
[7] Spadacini, C., Centemeri, L., Xodo, L., Astolfi, M., Romano, M., Macchi, E.. A new configuration for Organic Rankine C ycles power systems. In: First International Seminar on ORC Power Systems. 2011,.
[8] Persico, G., Pini, M., Dossena, V., Gaetani, P.. Aerodynamic Design and Analysis of Centrifugal Turbine Cascades. In: ASME Turbo Expo 2013. GT2013-95770; 2013,.
[9] Persico, G., Pini, M., Dossena, V., Gaetani, P.. Aerodynamics of Centrifugal Turbine Cascades. ASME J Eng Gas Turb Power 2015;137(112602):1–11.
[10] Peter, J., Dwight, R.. Numerical sensitivity analysis for aerodynamic optimization: A survey of approaches. Comput Fluids 2010;(39):373.
[11] Pini, M., Pasquale, D., Persico, G., Rebay, S.. Adjoint method for shape optimization in real-gas flow applications. ASME J Eng Gas Turb Power 2014;137:032604.
[12] Coello, C.. An updated survey of GA-based multiobjective optimization techniques. ACM Comput Surv 2000;32(2):109–143. doi:10.1145/358923.358929.
[13] Farin, G.. Curves and Surfaces for CAGD: A Practical Guide. 5th ed.; San Francisco, CA, USA: Morgan Kaufmann Publishers Inc.; 2002. ISBN 1-55860-737-4.
[14] Rodriguez-Fernandez, P., Persico, G.. Automatic Design of ORC Turbine Profiles Using Evolutionary Algorithms. In: 3rd International Seminar on ORC Power Systems. 133; 2015,.
[15] Colonna, P., Nannan, N., Guardone, A.. Multiparameter equations of state for siloxanes: $[(CH_3)_3\text{-Si-O}_{1/2}]_2\text{-}[O\text{-Si-}(CH_3)_2]_{i=1,3}$, and $[O\text{-Si-}(CH_3)_2]_6$. Fluid Ph Eq 2008;263:115–130.
[16] Persico, G., Mora, A., Gaetani, P., Savini, M.. Unsteady Aerodynamics of a Low Aspect Ratio Turbine Stage: Modeling Issues and Flow Physics. ASME J Turbomach 2012;134:061030 (10 pages).
[17] Reeves, C.R., Rowe, J.E.. Genetic Algorithms: Principles and Perspectives: A Guide to GA Theory. Norwell, MA, USA: Kluwer Academic Publishers; 2002. ISBN 1402072406.
[18] Persico, G.. Evolutionary Optimization of Centrifugal Nozzles for Organic Vapours. Journal of Physics: Conf Series 2017;821(012015):1–11.
[19] Adams, B.e.a.. Dakota, a multilevel parallel object-oriented framework for design optimization, parameter estimation, uncertainty quantification, and sensitivity analysis: Version 5.4 user's manual. Sandia Technical Report SAND2010-2183 2013;.
[20] Denos, R., Arts, T., Paniagua, G., Michelassi, V., Martelli, F.. Investigation of the Unsteady Aerodynamics in a Transonic Turbine Stage. ASME J Turbomach 2001;123(1):81–89.
[21] Miller, R., Moss, R., Ainsworth, R., Harvery, N.. Wake, Shock, and Potential Field Interactions in a 1.5 Stage TurbinePart I: Vane-Rotor and Rotor-Vane Interaction. ASME J Turbomach 2003;125(1):33–39.